HHS Public Access

Author manuscript

Cancer Discov. Author manuscript; available in PMC 2015 December 01.

Published in final edited form as:

Cancer Discov. 2015 June ; 5(6): 622–635. doi:10.1158/2159-8290.CD-14-0921.

The p53 Target Gene *Siva* Enables Non-Small Cell Lung Cancer Development

Jeanine L. Van Nostrand[1], **Alice Brisac**[4], **Stephano S. Mello**[1], **Suzanne B. R. Jacobs**[1], **Richard Luong**[2], and **Laura D. Attardi**[1,3,5]

[1]Division of Radiation and Cancer Biology, Department of Radiation Oncology, Stanford University School of Medicine, Stanford, California 94305, USA

[2]Department of Comparative Medicine, Stanford University School of Medicine, Stanford, California 94305, USA

[3]Department of Genetics, Stanford University School of Medicine, Stanford, California 94305, USA

[4]Department of Biology, Ecole Normale Supérieure of Lyon, 15 parvis René Descartes – BP 7000 69342 Lyon Cedex 07, France

Abstract

Although p53 transcriptional activation potential is critical for its ability to suppress cancer, the specific target genes involved in tumor suppression remain unclear. *Siva* is a p53 target gene essential for p53-dependent apoptosis, although it can also promote proliferation through inhibition of p53 in some settings. Thus, the role of SIVA in tumorigenesis remains unclear. Here, we seek to define the contribution of SIVA to tumorigenesis by generating *Siva* conditional knockout mice. Surprisingly, we find that SIVA loss inhibits non-small cell lung cancer (NSCLC) development, suggesting that SIVA facilitates tumorigenesis. Similarly, SIVA knockdown in mouse and human NSCLC cell lines decreases proliferation and transformation. Consistent with this pro-tumorigenic role for SIVA, high-level *SIVA* expression correlates with reduced NSCLC patient survival. SIVA acts independently of p53, and instead, stimulates mTOR signaling and metabolism in NSCLC cells. Thus, SIVA enables tumorigenesis in a p53-independent manner, revealing a potential new cancer therapy target.

Keywords

p53; Siva; Non-Small Cell Lung Cancer; metabolism

[5]Corresponding author: CCSR-South, Room 1255, 269 Campus Drive, Stanford, CA 94305-5152, Telephone: 650-725-8424, Fax: 650-723-7382, attardi@stanford.edu.

Competing interests statement: The authors declare that they have no competing financial interests.

Author Contributions: J.L.V.N. designed and carried out experiments, interpreted data, and wrote the manuscript. A.B. performed cell culture experiments and interpreted data. S.S.M performed bioinformatics analysis. S.B.R.J. designed and generated the *Siva* conditional knockout targeting vector. R.L. performed preliminary lung tumor analysis. L.D.A. designed experiments, interpreted data, and wrote the manuscript.

Introduction

The p53 transcription factor is a critical tumor suppressor, as evidenced by the observations that is it mutated in over half of all human cancers and that *p53* null mice develop cancer with 100% penetrance (1). p53 is a cellular stress sensor that triggers various cellular responses, including apoptosis, cell-cycle arrest, and autophagy (2, 3), in response to diverse stress signals, including DNA damage, hyperproliferative stimuli, and nutrient deprivation, as a measure to restrain tumorigenesis (1, 4). While activation of apoptosis helps to eliminate defective cells, induction of cell-cycle arrest and the associated DNA repair program helps to maintain the genetic integrity of cells and cell survival (2). p53 relies primarily on its function as a transcriptional activator to trigger these different responses through induction of a host of different target genes (1, 4). While the specific target genes involved in cell-cycle arrest and apoptosis have been well characterized, the p53 target genes critical for tumor suppression remain incompletely understood (4, 5). Intriguingly, although transcriptional activation potential is critical for p53-mediated tumor suppression, canonical p53 target genes, such as *p21 (Cdkn1a)*, *Puma (Bbc3)*, and *Noxa (Pmaip1)* are dispensable for tumor suppression (6–8). Thus, key mediators of p53 tumor suppressor activity remain to be identified.

SIVA is a pro-apoptotic protein originally identified by virtue of its interaction with CD27 and other death receptors (9, 10). It was subsequently shown to be a direct p53 target gene that is specifically upregulated to high levels during apoptosis relative to G_1 cell-cycle arrest (11, 12). In addition, SIVA plays an important role in p53-dependent apoptosis *in vitro*, as loss of SIVA in cerebellar granular neurons (CGNs) compromises DNA-damage-induced, p53-dependent apoptosis (11). Furthermore, overexpression of SIVA in CGNs, mouse embryonic fibroblasts (MEFs), and lymphocytes is sufficient to induce cell death (11, 13). In CGNs exposed to DNA damage, SIVA localizes to the plasma membrane and induces apoptosis in a manner dependent on BID and BAX/BAK (11), consistent with SIVA acting through both the extrinsic and intrinsic cell death pathways. This pro-apoptotic function suggests that SIVA may itself have tumor suppressor activity.

Beyond its role in restraining cellular expansion through apoptosis, several lines of evidence suggest that SIVA also promotes proliferation. For example, *Siva* is directly transcriptionally activated by E2F1, a protein essential for promoting cell cycle progression (12). In addition, SIVA has been reported to suppress p53 activity by stabilizing the interaction between MDM2 and p53, leading to increased p53 ubiquitination and degradation, and increased BrdU incorporation (14). SIVA can also act as an E3-ubiquitin ligase for the p53-activating protein $p19^{ARF}$, thereby promoting $p19^{ARF}$ degradation, and consequently provoking p53 destabilization and enhanced cellular proliferation (15). Thus, these studies collectively suggest that SIVA could play a tumor-promoting role.

To explore whether SIVA exerts a tumor-suppressive or tumor-promoting role downstream of p53, we assessed the effect of SIVA loss in a mouse model of oncogenic KRAS-driven non-small cell lung cancer (NSCLC) development, in which p53 plays a key role in suppressing malignant progression. Using *Siva* conditional knockout mice that we generated, we found that SIVA is necessary for efficient oncogenic KRAS-driven NSCLC

development. Subsequent analysis of SIVA function *in vitro* revealed that *Siva* knockdown dampens proliferation and transformation in both mouse and human NSCLC cell lines. The diminished proliferation and transformation upon SIVA knockdown are independent of p53, and instead are associated with decreased metabolic function. These findings indicate that SIVA plays a p53-independent role in enabling lung cancer development and suggest the possibility that it could ultimately be a target for cancer therapy.

Results

Generation of *Siva* Conditional Knockout Mice

To analyze the role of SIVA in tumorigenesis *in vivo*, we generated *Siva* conditional knockout mice. Mouse embryonic stem (ES) cells were targeted such that the entire *Siva* locus, comprising four exons, was flanked by a LoxP and a Lox-Puro-Lox cassette, ensuring complete deletion of the *Siva* gene (Fig. 1A). Proper targeting of ES cells was confirmed by Southern blot analysis using both 5′ and 3′ external probes (Fig. 1B), and two independent lines of mice were generated. These mice were crossed to CMV-Cre transgenic mice (16) and progeny were screened for the presence of either a *Siva* conditional (denoted floxed or fl) or *Siva* null allele. To confirm that the floxed *Siva* allele could be efficiently recombined to generate *Siva* null cells, mouse embryo fibroblasts (MEFs) derived from E13.5 $Siva^{fl/-}$ embryos were infected with Adenovirus expressing Cre recombinase (Ad-Cre), and DNA was harvested. PCR verified that the floxed *Siva* allele was efficiently recombined, thereby producing *Siva* null cells (Fig. 1C). Furthermore, analysis of progeny from crosses between mice heterozygous for the *Siva* null allele revealed embryonic lethality of *Siva* homozygous mutant animals, similar to that observed previously with mice homozygous for a *Siva* gene-trapped allele (manuscript in preparation, data not shown).

SIVA enables KRAS-induced lung tumorigenesis

To determine the role of SIVA in tumorigenesis, we chose a NSCLC model in which p53 has been shown to play a critical role in suppressing tumor progression (17). In this model, activated $KRAS^{G12D}$ drives the development of lung adenomas, which progress to adenocarcinomas in the absence of p53 (5, 17). We utilized $Kras^{LSL\text{-}G12D}$ mice, in which an upstream floxed transcriptional stop cassette (*Lox-Stop-Lox*) silences $KRAS^{G12D}$ expression until Cre recombinase is introduced. We generated cohorts of $Kras^{LSL\text{-}G12D};Siva^{+/+}$, $Kras^{LSL\text{-}G12D};Siva^{fl/+}$, $Kras^{LSL\text{-}G12D};Siva^{+/-}$, and $Kras^{LSL\text{-}G12D};Siva^{fl/-}$ mice, which we infected with Ad-Cre through intratracheal injection (18) to drive expression of $KRAS^{G12D}$ and excision of the *Siva* locus. Mice were subjected 18 weeks later to a quantitative analysis of tumor development (Fig. 2A). Surprisingly, histological analyses revealed fewer tumors, including both adenomas and adenocarcinomas, and reduced tumor burden (percent lung area comprising tumors) in $Kras^{LSL\text{-}G12D};Siva^{fl/-}$ mice than in $Kras^{LSL\text{-}G12D};Siva^{+/+}$ control mice. $Kras^{LSL\text{-}G12D};Siva^{fl/-}$ mice also had reduced burden of hyperplastic lesions compared to controls (Fig. 2B–E). In addition, we observed reduced tumor number and tumor burden in *Siva* heterozygous mice ($Kras^{LSL\text{-}G12D};Siva^{fl/+}$, $Kras^{LSL\text{-}G12D};Siva^{+/-}$) relative to $Kras^{LSL\text{-}G12D};Siva^{+/+}$ controls (Supplemental Fig. 1A–B). Furthermore, the tumor burden and tumor number in $Kras^{LSL\text{-}G12D};Siva$-heterozygous mice is comparable to that observed

in *Kras*$^{LSL\text{-}G12D}$;*Siva*$^{fl/-}$ mice. Together, these observations indicate that SIVA loss impedes tumor initiation, and that SIVA normally enables tumorigenesis.

Siva knockdown inhibits mouse NSCLC cell proliferation

To explore the mechanisms underlying the decreased tumorigenesis observed following SIVA inactivation, we utilized two mouse NSCLC cell lines, LSZ2 and LSZ4, generated previously by serial allograft passage of tumors derived from *Kras*^{G12D};*p53*$^{+/+}$ mice. Importantly, these tumor cells still harbor wild-type p53 (19) and express SIVA (Fig. 3A). We used two independent shRNAs directed against *Siva* and achieved a 70–80% reduction in SIVA protein levels following lentiviral transduction with each (Fig. 3A). We first analyzed the proliferative capacity of cells upon *Siva* knockdown, by assessing BrdU incorporation. Perturbation with either *Siva* shRNA resulted in a significant decrease in the percentage of BrdU-positive cells in both cell lines relative to control GFP shRNA (Fig. 3B), indicating that SIVA facilitates proliferation. In contrast, depleting SIVA by infecting *Siva*$^{fl/-}$ MEFs with Adeno-Cre or knocking-down Siva in pancreatic cancer cell lines did not affect the proliferative index (Supplemental Fig. 2A-B), suggesting that SIVA's role in facilitating proliferation is cell type- or context-specific. Notably, *Siva* knockdown in LSZ-4 cells did not augment the percentage of Annexin V-positive cells, indicating that increased apoptosis is not responsible for diminished tumor burden (Supplemental Figure 3A–B). Next, to more directly explore whether *Siva* knockdown affects the transformation properties of NSCLC cells, we assessed the ability of cells to form colonies upon low-density plating and upon anchorage-independent growth in soft agar. *Siva* knockdown resulted in fewer colonies forming in the low-density plating assay compared to *shGFP* control-expressing cells (Fig. 3C). Similarly, using a soft agar assay, fewer colonies were able to form upon *Siva* knockdown than with *shLacZ* control shRNA (Fig. 3D). Together, these results suggest that SIVA enhances proliferation and transformation, thus recapitulating our findings in the *in vivo* tumorigenesis study.

SIVA knockdown inhibits human NSCLC cell proliferation

To determine whether the role for SIVA in promoting efficient tumorigenesis in mouse cells is conserved in human cells, we next examined whether SIVA similarly facilitates the proliferation of human A549 NSCLC cells expressing oncogenic KRAS^{G12S} and wild-type p53. We knocked-down *Siva* in A549 cells using lentiviral transduction of *Siva* shRNAs and observed depletion of *Siva* mRNA by quantitative RT-PCR (Fig. 4A). We assessed the importance of SIVA for cellular proliferation by generating growth curves and measuring BrdU incorporation. As observed in the mouse LSZ4 and LSZ2 cell lines, *Siva* knockdown in A549 cells results in reduced proliferative potential relative to the shGFP control (Fig. 4B–C). Furthermore, knockdown of *Siva* inhibited colony formation in both low-density plating and soft agar assays relative to the *shGFP* control, revealing an important role for SIVA in promoting transformation (Fig. 4D–E). These results demonstrate that SIVA not only enhances proliferation and transformation in mouse NSCLC cells but also in human NSCLC cells. Supporting the idea that *Siva* expression can promote tumorigenesis, analysis of survival data for human NSCLC patients revealed that patients with lung cancers expressing high levels of *SIVA* have significantly reduced overall survival than those with

lung cancers expressing low levels of *Siva* (20, 21) (Fig. 4F). Thus, *Siva* expression levels have prognostic power in human NSCLC patients.

Siva knockdown inhibits proliferation and transformation in a p53-independent manner

Decreased proliferative capacity and suppression of transformation ability are well-known effects of p53 activation. It has been previously reported that SIVA can negatively regulate p53 by stabilizing the p53-MDM2 interaction and by promoting $p19^{ARF}$ degradation and that SIVA loss can therefore induce p53 activity (14, 15). We therefore sought to test whether stabilization and activation of p53 provokes the inhibition of proliferation and transformation we observed upon SIVA inactivation in NSCLC cells. First, we assessed p53 protein levels and activity upon *Siva* knockdown in LSZ4 cells. Western blot analysis of p53 in LSZ4 cells after *Siva* knockdown revealed no difference in p53 levels, despite a clear inhibition of proliferation (Fig. 5A). Second, since p53 is a transcriptional activator, we analyzed p53 target gene expression as a readout of p53 activity. Upon *Siva* knockdown in LSZ4 cells, we observed no difference in p53 target gene expression relative to *shGFP*-expressing cells, suggesting that SIVA does not stimulate proliferation in NSCLC cell lines by inactivating p53, as previously described (Fig. 5B). Finally, we investigated whether p53 is required for the phenotypic effects of *Siva* knockdown. Upon attenuation of both *p53* and *Siva* in LSZ4 cells using RNA interference, we assessed BrdU incorporation and found that additional knockdown of p53 does not rescue the inhibition of proliferation triggered by SIVA loss (Fig. 5C–E) These results were bolstered by analysis of p53-null NSCLC cell lines, where we observed that *Siva* knockdown also causes decreased transformation in soft agar assays, similarly to *Siva* knockdown in p53-expressing LSZ4 cells (Fig. 5F). Thus, the inhibition of proliferation caused by attenuated *Siva* expression does not rely on p53.

Siva knockdown alters expression of metabolic genes

To gain an understanding of the molecular basis for the reduced proliferation and transformation resulting from *Siva* knockdown, we performed gene expression profiling experiments on LSZ4 and LSZ2 cells after *Siva* knockdown by lentiviral transduction with each of the two previously characterized shRNAs (*shSiva1* and *shSiva2*) and each of two control shRNAs (*shLacZ* and *shGFP*). Hierarchical clustering revealed a notable difference in gene expression profiles between *Siva* knockdown and control samples (Fig. 6A). Differentially expressed genes were analyzed for enrichment in Gene Ontology (GO) terms using GeneSpring Analysis. We found that the most enriched GO terms included immune regulation – consistent with SIVA's known role in regulating NFκB signaling – as well as cell migration and metabolic processes (Fig. 6B). We first queried whether altered NFκB signaling could be responsible for the decreased proliferation upon *Siva* loss by western blot analysis of activated p65, a component of canonical NFκB (22) signaling. However, neither p65 nor phospho-p65 levels were altered upon *Siva* knockdown in LSZ-4 cells (Supplemental Fig. 4A). Moreover, although SIVA has been shown to impinge upon NFκB signaling through inhibition of the TGF-β Activated Kinase 1 (TAK1) (23), we found that pharmacological TAK1 inhibition (22) was not able to rescue the reduced proliferation caused by *Siva* knockdown (Supplemental Fig. 4B). These findings suggest that the known role of SIVA in NFκB signaling does not account for the pro-tumorigenic effects of SIVA. Thus, given the critical role for the appropriate regulation of metabolism in cancer cell

proliferation and survival, we next sought to investigate a potential role for SIVA in regulating metabolism.

Siva knockdown decreases metabolic activity and induces autophagy

To interrogate the role of SIVA in regulating metabolism, we first examined whether metabolic function is altered upon *Siva* knockdown by measuring oxygen consumption rates (OCR) and extracellular acidification rates (ECAR), as indicators of oxidative phosphorylation and glycolytic rates, respectively. These analyses revealed that knockdown of *Siva* in both LSZ4 and LSZ2 cells decreases mitochondrial respiration and, less dramatically, glycolysis, suggesting an overall reduction in metabolic function (Fig. 6C and data not shown). Specifically, while the basal oxidative phosphorylation rate was reduced slightly upon *Siva* knockdown, the maximal mitochondrial respiration capacity, measured upon treatment with the ATP synthesis-electron transport uncoupler FCCP, was significantly decreased upon *Siva* knockdown. Treatment with either oligomycin – an ATP synthase inhibitor that reveals the OCR associated with mitochondrial proton leak – or antimycin – a cytochrome C inhibitor that disrupts the proton gradient and reveals mitochondrial-independent respiration – did not cause any significant change in oxygen consumption rate upon SIVA inhibition, suggesting a specific role for SIVA in mitochondrial metabolism. To investigate why mitochondrial function is decreased upon *Siva* knockdown, we examined mitochondrial content by quantifying mitochondrial DNA, specifically the mitochondrial *Cox 3*, *Cyt B*, and *16S* rRNA genes. Quantitative PCR revealed that mitochondrial DNA content is reduced by approximately 40% in both LSZ2 and LSZ4 cells upon *Siva* knockdown, providing a basis for the decreased mitochondrial respiration function (Fig. 6D). These results suggest that SIVA is critical for promoting efficient metabolism through the mitochondria, and thus SIVA may normally promote proliferation by facilitating efficacious ATP production.

An important homeostatic response of cells to decreased energy production is to induce autophagy, a process by which organelles and cytoplasmic proteins are degraded either for energy production or quality control. We therefore sought to query whether autophagy might be induced upon *Siva* knockdown. We assessed levels of autophagy by immunoblotting for modified LC3 (LC3-II), which is converted from LC3-I upon conjugation of phosphatidylethanolamine and then incorporated into autophagic vesicles, thus serving as a marker of autophagy. To confirm that any enhanced LC3-II signal represents increased autophagic flux rather than a block in autophagy resulting in accumulation of autophagosomes, we also analyzed cells treated with Bafilomycin A1 (Baf), an inhibitor of autophagic vesicle maturation. We observed an increase in LC3-II levels upon *Siva* knockdown relative to the shGFP control, which was further enhanced with Baf treatment, indicating that SIVA inhibition triggers increased autophagic flux (Fig. 6E). To determine if the increased autophagy associated with *Siva* knockdown could be responsible for decreasing proliferation, as occurs with AMBRA1 or UVRAG overexpression (24, 25), we inhibited autophagy using chloroquine and analyzed BrdU incorporation in Siva knockdown cells. Inhibition of autophagy was indeed able to partially rescue the dampened proliferation upon *Siva* knockdown (Fig. 6F), suggesting that the increased autophagy contributes to the reduced proliferation and tumorigenic potential upon Siva loss. We also observed that

inhibition of autophagy decreased proliferation in control cells, suggesting that efficient proliferation relies on some level of autophagy. These observations collectively suggest that SIVA normally suppresses autophagy, possibly either indirectly by maintaining proper energy production or directly by negatively regulating an upstream signaling pathway triggering autophagy.

SIVA enhances mTOR activity

To gain insight into the molecular underpinnings of SIVA function in metabolism and autophagy, we examined signaling pathways through which SIVA might act. We first analyzed the genes modulated upon *Siva* knockdown using Gene Set Enrichment Analysis (GSEA) and found an enrichment for signatures associated with decreased proliferation, occurring with diminished KRAS, E2F1, and mTOR signaling or increased RB activity (Fig. 7A). We also identified signatures associated with increased NFκB signaling (TBK1 activation; KRAS.DF.V1_DN) (26), decreased ribosomal function (RPS14_DN.V1_UP), and decreased chromatin remodeling activity/histone modification (BMI1_DN.V1_UP). We found mTOR signaling a particularly compelling pathway to pursue given the numerous parallels seen between SIVA and mTOR, which also has a known role in regulating mitochondrial metabolism, inhibiting autophagy, promoting cell proliferation, and supporting tumorigenesis (27). These observations, coupled with our finding that *Siva* knockdown produces a signature resembling those associated with decreased mTOR signaling suggest that SIVA may promote mTOR signaling (Fig. 7B). To test this hypothesis, we first examined whether *Siva* knockdown results in decreased mTOR activity by analyzing phosphorylation of the mTOR substrates S6 kinase (S6K) and 4EBP1 as well as the S6K substrate S6. Indeed, we observed a reduction in Phospho-S6K, Phospho-S6, and Phospho-4EBP1 levels upon *Siva* knockdown, indicative of diminished mTOR activity, consistent with the gene expression data (Fig. 7C). These findings indicate that SIVA is indeed necessary for full mTOR activity. We next examined whether reduced mTOR activity results in diminished proliferation in LSZ-4 cells. We used two mTOR inhibitors, Torin1 and Rapamycin, which target mTOR complex 1 and both mTOR complexes 1 and 2, respectively, and quantified the rate of BrdU incorporation. Similarly to *Siva* knockdown, inhibition of mTOR activity significantly decreased proliferation of LSZ-4 cells, suggesting that mTOR activity is indeed necessary for maximal LSZ-4 cell proliferation (Fig. 7D).

mTOR is regulated either by AMPK, which inhibits mTOR activity through phosphorylation and inhibition of RAPTOR at S722/S792 and phosphorylation and activation of TSC2 at S1387, or by mitogenic signaling pathways, which activate mTOR by phosphorylating and inhibiting TSC2 at S1462 (27). To determine how Siva inhibits mTOR activity, we examined the phosphorylation of RAPTOR at serine 792, as a marker of AMPK signaling, and phosphorylation of TSC2 at serine 1462, as a marker of mitogenic signaling pathways. While we observed no difference in phospho-RAPTOR levels in cells with different *Siva* status, we observed a decrease in phospho-S1462 TSC2 levels upon *Siva* knockdown, suggesting that SIVA acts through mitogenic signaling rather than AMPK signaling to promote mTOR activity (Fig. 7E). Together, these findings reveal that SIVA is essential for maximal mTOR activity, which is necessary for optimal proliferation in LSZ-4 cells.

To determine whether decreased mTOR activity is responsible for the proliferation defects upon *Siva* knockdown, we tested whether reactivation of mTOR signaling through knockdown of TSC2 could rescue BrdU incorporation in shSiva-transduced cells. Indeed, with approximately 50% knockdown of *Tsc2*, we observed a partial rescue in BrdU incorporation in shSiva-transduced cells and no effect in control cells (Fig. 7F). Collectively, these findings reveal a novel role for SIVA in promoting mTOR activity and metabolism, which is necessary for enhancing proliferation and tumorigenesis downstream of oncogenic KRAS (Fig. 7G).

Discussion

Here, we describe a critical role for the p53 target gene *Siva* in facilitating NSCLC development. Conditional inactivation of *Siva* in an autochthonous oncogenic $Kras^{G12D}$-driven model for NSCLC resulted in decreased tumor numbers and tumor burden relative to SIVA-expressing controls. Moreover, we found that *Siva* knockdown inhibits proliferation and transformation in both mouse and human NSCLC cells *in vitro*. We discovered further that SIVA does not exert its pro-tumorigenic effect by restraining p53. Instead the enhancement of tumorigenesis by SIVA relates to its ability to promote mTOR signaling, inhibit autophagy and augment metabolic activity (28–30). Consistent with this pro-tumorigenic role, high-level *SIVA* expression correlates with worse prognosis in NSCLC patients (20).

Previous reports showed that SIVA loss promotes p53 stabilization and inhibits proliferation, attributable to SIVA function in enabling p53-MDM2 interactions and in enhancing ubiquitin-mediated ARF degradation (14, 15). In contrast, we found that p53 activation is not responsible for the inhibition of proliferation upon SIVA loss, as p53 was not induced upon *Siva* attenuation and *Siva* knockdown could inhibit proliferation and transformation irrespective of *p53* status. However, the observation that SIVA is able to promote tumorigenesis reveals an intriguing contradiction with respect to its role as a p53 target gene, perhaps reflecting the fact that p53 target genes are often regulated by additional transcription factors and function in a p53-independent manner in some contexts. For example, SIVA can also be induced by the E2F1 transcription factor, which can play both tumor suppressive and oncogenic roles (12, 31). Such a pro-tumorigenic role of a p53 target gene recalls *TIGAR*, a p53 target gene involved in cell survival upon oxidative stress, which promotes tumorigenesis in a mouse small intestinal cancer model (32). Moreover, TIGAR is thought to be upregulated in a p53-independent manner in human tumors (33). Our work similarly suggests that SIVA plays a p53-independent role in promoting proliferation and tumorigenesis.

Although SIVA clearly alters the metabolic capacity of NSCLC cells, reflected by enhanced mitochondrial respiration and reduced autophagy, it remains unclear how precisely SIVA exerts these effects. SIVA may affect metabolism by stimulating mTOR signaling, which is known to enhance oxidative metabolism at least in part via activation of S6K and 4EBP1 and consequent translation of nuclear-encoded mitochondrial proteins (34, 35), and to dampen autophagy through phosphorylation and inactivation of the autophagy initiating kinase ULK1/ATG1 (36). Moreover, mTOR is known to promote tumorigenesis in mouse

hepatocellular, renal and lung cancer models (28, 29, 37, 38). Thus, a role for SIVA in the positive regulation of mTOR could account for the decreased oxidative phosphorylation, increased autophagy, and reduced tumor burden with *Siva* deficiency (27, 34, 36, 38). Based on our western blot analyses of upstream signaling pathway components, SIVA appears to exert effects on mTOR signaling not through the negative regulator AMPK, which responds to cellular energy levels, but rather through positively regulating mitogenic signaling pathways, such as the ERK1/2, WNT, and AKT signaling pathways, which respond to growth signals (27, 37). However, the exact mechanisms by which SIVA activates these mitogenic signaling pathways and which mitogenic signaling pathways are most important remain to be elucidated.

An alternative mechanism for SIVA action is that it affects metabolism through pathways related to its apoptotic function. A precedent for this notion comes from the observation that loss of both BAX and BAK, which renders cells completely apoptosis-deficient, triggers increased autophagy and decreased mTOR signaling in response to stress signals, as a measure to maintain cell viability (39, 40). Loss of SIVA could similarly promote autophagy in the presence of a stress signal such as oncogenic KRAS. That SIVA loss could mimic BAX/BAK deficiency is consistent with the observation that BAX and BAK are required for SIVA to induce apoptosis (11). A role for SIVA at the mitochondria is further supported by the decreased mitochondrial function observed upon SIVA knockdown. Interestingly, mitochondrial respiration has been found to be required for mitochondrial apoptosis by allowing for efficient mitochondrial depolarization and release of pro-apoptotic factors (41, 42). Thus, diminished mitochondrial respiration may be a mechanism by which *Siva*-deficiency protects cells from apoptosis, in keeping with the important role for Siva in apoptosis (11). Overall, elucidating the mechanisms through which SIVA deficiency inhibits mTOR signaling, dampens OXHPOS, and triggers autophagy will be an important future goal for understanding how SIVA promotes tumorigenesis.

In addition to defining a role for SIVA in efficient mTOR signaling, we also identified additional signaling pathways affected by SIVA status in our microarray experiments. One particularly interesting signaling pathway upregulated upon Siva knockdown is the TBK1 pathway. TBK1 is an IKB kinase that promotes survival through the NFκB and AKT pathways and is required for KRAS-dependent NSCLC proliferation. (26, 43). However, TBK1 has also been shown to inhibit mTOR activity and promote autophagy (44). Thus, while upregulation of TBK1 signaling could explain how *Siva*-deficiency inhibits mTOR activity and drives autophagy, the pro-proliferative activity attributed to activated TBK1 contrasts with the decreased proliferation observed upon SIVA inactivation, suggesting that TBK1 is not a primary SIVA mediator. Another intriguing signature associated with Siva knockdown is activated HIPPO-YAP signaling. The YAP pathway controls organ size and tumorigenesis by promoting cell proliferation and inhibiting apoptosis (45). Moreover, YAP activates the P13K-mTOR pathway by inhibiting PTEN (37, 46). Therefore, it is possible that Siva activates the mTOR pathway by activating the YAP pathway. Another signature identified upon Siva knockdown is that of inhibition of BMI1, a component of the polycomb repressive complex, which promotes both cell self-renewal and tumorigenesis (47). While loss of BMI1 results in decreased tumorigenic potential and decreased mitochondrial

oxidative capacity, like SIVA loss, it is not known to promote other phenotypes associated with SIVA deficiency, such as inhibition of mTOR signaling (48). It will be of great interest in future studies to further evaluate the role of SIVA in these additional signaling pathways to better define the mechanisms by which SIVA promotes tumorigenesis.

Our findings that SIVA is necessary for efficient tumorigenesis in an autochthonous lung cancer model suggests the possibility of SIVA as a therapeutic target. Indeed, the pro-tumorigenic role of SIVA is supported by a previous xenograft study in which *SIVA* knockdown in U2OS cells was found to inhibit tumor growth relative to control knockdown cells (14). Furthermore, our finding that alternate cell types, including primary MEFs, are not adversely affected by SIVA loss suggests that SIVA inhibition could represent a useful strategy for cancer treatment. In future studies, it will also be interesting to further elaborate the role of SIVA *in vivo* using mouse models for other cancer types to determine whether SIVA generally plays an enabling role in tumorigenesis or if SIVA might play context-dependent roles in cancer development, sometimes suppressing tumor development. Regardless, the discovery of a role for SIVA in enhancing tumorigenesis unveils a potential new therapeutic target for cancer treatment.

METHODS

Generation of *Siva* Conditional Knockout Mice

The *Siva* locus was isolated from a BAC clone, 122D14, obtained from the Sanger Institute, using BspE1 and BstE11 restriction enzymes. The fragment including *Siva* was modified to incorporate a 5′ LoxP site at the BspE1 site and a 3′ Lox-PGK-Puro-Lox cassette at the BstE11 site and subcloned into the 184-DT-PL vector. The *Siva* targeting construct was introduced into J1 ES cells by electroporation. ES cells were cultured on irradiated MEF feeders in LIF-containing media (Millipore). Positive clones were identified by PCR and Southern blot analysis for both 5′ and 3′ targeting and used to generate chimeric mice at the Stanford transgenic research facility. Chimeras were bred to C57BL/6 females and progeny genotyped by Southern blot analysis or PCR as described below. Mice were further bred to CMV-Cre mice to excise the Puro cassette, resulting in a single LoxP site 3′ of the *Siva* locus ($Siva^{fl}$). For analysis, *Siva* conditional mice were bred to $Kras^{LSL\text{-}G12D/+}$ mice. All animal work was done in accordance with the Stanford University APLAC.

Genotyping

Genotyping was performed by PCR analysis of tail DNA. The primers used include a forward primer 5′ for the LoxP site (F1: AGT ACC AGC ATT CCC TGG TG), a reverse primer 3′ to the LoxP site (R1: GGA GTC AGA CCT CGT TAC GG), and a reverse primer 3′ to the LoxPuroLox site (R2: CCA CAC AGG ACA TTC CAC AG).

Lung Tumor Analysis

For the tumor study, mice were intratracheally injected with 4 × 10^6 PFU of Ad-Cre (University of Iowa GTVR), as described (18). Mice were sacrificed 18 weeks later for analysis of tumor number and burden. Lungs were paraformaldehyde-fixed, each lobe bi- or

tri-sected, and paraffin-embedded. Histological analysis was performed on hematoxylin and eosin-stained sections. Lung area and tumor area were quantified using ImageJ.

Cell Culture

LSZ2, LSZ4, A549, *p53*-null NSCLC cells, and MEFs were cultured in DMEM with 10% serum (3, 19). LSZ2 and LSZ4 cells were a gift from Alejandro Sweet-Cordero (Stanford School of Medicine, Stanford, California). *p53* status was confirmed by western blot and target gene expression analyses but cell lines were not otherwise authenticated. *p53*-null NSCLC cells were derived from $Kras^{LA2}$;*p53*-null mice as described (3). Mouse embryonic fibroblasts (MEFs) were derived from wild-type or $Siva^{fl/-}$ E13.5 embryos and genotypes determined by PCR. Cells were last tested for mycoplasma using Lonza MycoAlert Assay (LT07-118) at time of revisions. Adenoviral infections were performed at an MOI of ~100 using adenoviral Cre or empty (Ad-Cre or Ad-Emp, University of Iowa GTVR) for 24 hours. Cells were imaged using phase contrast microscopy. For BrdU incorporation analysis, cells were incubated with 3μg/ml BrdU for 4 hours before fixation of cells on coverslips using 4% paraformaldehyde. Cells were treated with 50nM Rapamycin, 50nM Torin1, or 100nM Chloroquine for 18 hours prior to the BrdU pulse. TSC2 was knocked-down with Dharmacon smart pool siRNAs (Cat. #L-047050-00) using Lipofectamine RNAiMax reagent (Life Technology) and cells were BrdU pulsed 72 hours later. Immunofluorescence was performed as described with anti-BrdU antibody (1:50, 347580, BD Bioscience) (5). Proliferation was monitored using a Sulforhodamine B assay as described (49) on trichloroacetic acid-fixed cells collected every two days over a seven day period. For low plating assays, 150 cells were plated into 6 well dishes, collected ten days later, and colonies were stained with crystal violet. For soft agar assays, 10^5 cells were cultured in 2.4% noble agar in DMEM with 10% serum for two or three weeks. Colonies were visualized after staining with 0.02% Giemsa and quantified using Image J on scanned images. For respiration rate analysis, 10^4 cells were plated in each well of a 96 well plate and analyzed for the oxygen consumption and extracellular acidification rates on an XF96 Extracellular Flux Analyzer (Seahorse Biosciences) upon treatment with oligomycin, FCCP, or antimycin. Rates were normalized to cell number.

Western Blot Analysis

Cells were collected and lysed with RIPA buffer (1% NP40, 0.5% Sodium Deoxycholate, 0.1% SDS, Tris pH8.0) with protease inhibitors (Complete, Roche) or SDS Buffer (20% SDS, Tris pH6.8) with protease and phosphatase inhibitors (Roche). Western blots were probed with anti-p53 (1:500 CM5, Vector Labs), anti-LC3 (1:2000, NB100-2220, Novus), anti-S6K (1:1000, 9206, Cell Signaling Technology), anti-P-S6k (1:1000, 2708, Cell Signaling Technology), anti-4EBP1 (1:1000, 9452, Cell Signaling Technology), anti-P-4EBP1 (1:1000, 9459, Cell Signaling Technology), anti-SIVA (1:500, J.V.N, see below), anti-phospho-S6 (1:1000, 4858, Cell Signaling Technology), anti-S6 (1:1000, 2217, Cell Signaling Technology), anti-phospho-RAPTOR (1:1000, 2083, Cell Signaling Technology), anti-RAPTOR (1:1000, 2280, Cell Signaling Technology), anti-phospho-TSC2 (1:1000, 3617, Cell Signaling Technology), anti-TSC2 (1:1000, 3612, Cell Signaling Technology), anti-PARP (1:1000, 9532, Cell Signaling Technology) or anti-ACTIN (1:30,000 Sigma

A2228). SIVA antibodies were generated by injecting rabbits with a recombinant mouse MBP-SIVA fusion protein and purified using recombinant GST-SIVA.

qPCR

For qRT-PCR, NSCLC cells were cultured at subconfluency, RNA was isolated by Trizol extraction and reverse transcribed using MMLV reverse transcriptase (Invitrogen) and random primers, and PCR was performed in triplicate using SYBR green (Qiagen, Bio-Rad) and specific primers for each gene (Supplemental Table 1) in a 7900HT Fast Real-Time PCR machine (Applied Biosystems). Results were computed relative to a standard curve made with cDNA pooled from all samples and normalized to *β-Actin*. For qPCR of mitochondrial DNA, NSCLC cells were cultured at subconfluency, cells were lysed in RIPA buffer with Proteinase K, and DNA was purified with phenol/chloroform extraction followed by ethanol precipitation. PCR was performed in triplicate using SYBR green (Qiagen, Bio-Rad) and mouse-specific primers for each mitochondrial gene. Results were computed relative to a standard curve made with DNA pooled from all samples and normalized to *β2-microglobulin*.

Microarray Analysis

Microarray analysis was performed on RNA isolated by Trizol extraction from LSZ2 and LSZ4 cells transduced with two independent *Siva* shRNAs (shSiva1 and shSiva2) or two control shRNAs (shGFP and shLacZ). RNA was hybridized to Agilent Sureprint G3 Mouse GE 8 × 60K microarrays (G4852A) by the Stanford Functional Genomics Facility (microarray data files were deposited at Gene Expression Omnibus: GSE66126) and data were normalized and analyzed using GeneSpring GX software (Agilent). Gene ontology annotation was performed using GeneSpring GX software, and Gene Set Enrichment Analysis (GSEA) was performed using GSEA software (50).

Constructs

Siva knockdown was performed using two independent mouse shRNAs: LL37-GFP shSiva1 (GAGCGAAGATTGTTCCGTGAA, Broad Institute) or pLKO TRC2 shSiva1 (GATTGTTCCGTGAACCACC) and pLKO TRC2 shSiva2 (GGGCCTATAGAGATCACATAT); and one human shRNA: pLKO TRC2 shSiva (GCTACAGCTCAAGGTCCGCGTC). *p53* knockdown was performed using an shRNA: LMN shp53 (CCCACTACAAGTACATGTGTAA). pLKO TRC2 shGFP, LMN shLuc, or LL37-GFP shLacz were used as negative controls.

Supplementary Material

Refer to Web version on PubMed Central for supplementary material.

Acknowledgments

This work was supported by funding from the NSF and NCI (Grant Number 1F31CA167917-01) to JLVN and by funding from the ACS, LLS, and NIH (RO1 CA140875) to LDA.

We thank R.J. Shaw for reading the manuscript and S.E. Artandi for discussion. We thank A. Sweet-Cordero for LSZ2 and LSZ4 cell lines, K.T. Bieging for the *p53*-null NSCLC cell line and *p53* shRNA construct, and N.

Bardeesy for pancreatic cancer cell lines. We thank A. Flore for technical assistance with intratracheal injections for the lung tumor study. We thank L. Johnson and O. Foreman for assistance with histological analysis of tumors. We thank the Stanford Functional Genomics Facility for assistance with microarray analysis and Agilent for providing microarrays, E. LaGory for assistance with the Seahorse Analyzer, and R. Shaw, A. Giaccia, and A. Brunet for mTOR pathway antibodies and reagents.

Abbreviations

NSCLC	non-small cell lung cancer
MEF	mouse embryo fibroblast
OCR	oxygen consumption rate
ECAR	extracellular acidification rate
OXPHOS	oxidative phosphorylation

References

1. Vousden KH, Prives C. Blinded By The Light: The Growing Complexity of p53. Cell. 2009; 137(3): 413–31. [PubMed: 19410540]
2. Carvajal LA, Manfredi JJ. Another Fork in the Road—Life Or Death Decisions by the Tumour Suppressor p53. Embo Rep. 2013; 14(5):414–21. [PubMed: 23588418]
3. Kenzelmann Broz D, Mello SS, Bieging KT, Jiang D, Dusek RL, Brady CA, et al. Global Genomic Profiling Reveals an Extensive p53-Regulated Autophagy Program Contributing to Key p53 Responses. Genes & Development. 2013; 27(9):1016–31. [PubMed: 23651856]
4. Bieging KT, Mello SS, Attardi LD. Unravelling Mechanisms of p53-Mediated Tumour Suppression. Nature Reviews. 2014; 14(5):359–70.
5. Brady CA, Jiang D, Mello SS, Johnson TM, Jarvis LA, Kozak MM, et al. Distinct p53 Transcriptional Programs Dictate Acute DNA-Damage Responses and Tumor Suppression. Cell. 2011; 145(4):571–83.10.1016/J.Cell.2011.03035 [PubMed: 21565614]
6. Valente LJ, Gray Daniel HD, Michalak EM, Pinon-Hofbauer J, Egle A, Scott Clare L, et al. p53 Efficiently Suppresses Tumor Development in the Complete Absence of Its Cell-Cycle Inhibitory and Proapoptotic Effectors p21, Puma, And Noxa. Cell Reports. 2013; 3(5):1339–45. [PubMed: 23665218]
7. Timofeev O, Schlereth K, Wanzel M, Braun A, Nieswandt B, Pagenstecher A, et al. p53 DNA Binding Cooperativity Is Essential for Apoptosis and Tumor Suppression In Vivo. Cell Reports. 2013; 3(5):1512–25. [PubMed: 23665223]
8. Li T, Kon N, Jiang L, Tan M, Ludwig T, Zhao Y, et al. Tumor Suppression in the Absence of p53-Mediated Cell-Cycle Arrest, Apoptosis, and Senescence. Cell. 2012; 149(6):1269–83. [PubMed: 22682249]
9. Prasad KV, Ao Z, Yoon Y, Wu MX, Rizk M, Jacquot S, et al. CD27, a Member of the Tumor Necrosis Factor Receptor Family, Induces Apoptosis and Binds to Siva, a Proapoptotic Protein. Proceedings Of The National Academy Of Sciences. 1997; 94(12):6346–51.
10. Spinicelli S, Nocentini G, Ronchetti S, Krausz LT, Bianchini R, Riccardi C. GITR Interacts with the Pro-Apoptotic Protein Siva and Induces Apoptosis. Cell Death Differ. 2002; 9(12):1382–4. [PubMed: 12478477]
11. Jacobs S, Basak S, Murray JL, Pathak N, Attardi LD. Siva Is an Apoptosis-Selective p53 Target Gene Important for Neuronal Cell Death. Cell Death Differ. 2007; 14:1374–85. [PubMed: 17464332]
12. Fortin A, Maclaurin JG, Arbour N, Cregan SP, Kushwaha N, Callaghan SM, et al. The Proapoptotic Gene Siva Is a Direct Transcriptional Target for the Tumor Suppressors p53 And E2F1. J Biol Chem. 2004; 279(27):28706–14. [PubMed: 15105421]

13. Py B, Slomianny C, Auberger P, Petit PX, Benichou S. Siva-1 and an Alternate Splice Form Lacking the Death Domain, Siva-2, Similarly Induce Apoptosis in T Lymphocytes Via a Caspase-Dependent Mitochondrial Pathway. J Immunol. 2004; 172(7):4008–17. [PubMed: 15034012]
14. Du W, Jiang P, Li N, Mei Y, Wang X, Wen L, Yang X, Wu M. Suppression of p53 Activity by Siva1. Cell Death And Differentiation. 2009; 16(11):1493–504. [PubMed: 19590512]
15. Wang X, Zha M, Zhao X, Jiang P, Du W, Tam A, et al. Siva1 Inhibits p53 Function by Acting as an Arf E3 Ubiquitin Ligase. Nat Commun. 2013; 4:1551.10.1038/Ncomms2533 [PubMed: 23462994]
16. Hildebrandt T, Preiherr J, Tarbe N, Klostermann S, Van Muijen GN, Weidle UH. Identification of THW, a Putative New Tumor Suppressor Gene. Anticancer Research. 2000; 20:2801–9. [PubMed: 11062687]
17. Jackson EL, Olive KP, Tuveson DA, Bronson R, Crowley D, Brown M, et al. The Differential Effects of Mutant p53 Alleles on Advanced Murine Lung Cancer. Cancer Research. 2005; 65(22): 10280–8. [PubMed: 16288016]
18. Dupage M, Dooley AL, Jacks T. Conditional Mouse Lung Cancer Models Using Adenoviral or Lentiviral Delivery of Cre Recombinase. Nat Protocols. 2009; 4(8):1064–72.10.1038/Nprot.200995
19. Vicent S, Sayles LC, Vaka D, Khatri P, Gevaert O, Chen R, et al. Cross-Species Functional Analysis of Cancer-Associated Fibroblasts Identifies a Critical Role for Clcf1 and Il-6 in Non–Small Cell Lung Cancer In Vivo. Cancer Research. 2012; 72(22):5744–56. [PubMed: 22962265]
20. Győrffy B, Lánczky A, Szállási Z. Implementing an Online Tool for Genome-Wide Validation of Survival-Associated Biomarkers in Ovarian-Cancer Using Microarray Data from 1287 Patients. Endocrine-Related Cancer. 2012; 19(2):197–208. [PubMed: 22277193]
21. Győrffy B, Surowiak P, Budczies J, Lánczky A. Online Survival Analysis Software to Assess the Prognostic Value of Biomarkers Using Transcriptomic Data in Non-Small-Cell Lung Cancer. Plos One. 2013; 8(12):E82241. [PubMed: 24367507]
22. Wu J, Powell F, Larsen NA, Lai Z, Byth KF, Read J, et al. Mechanism and In Vitro Pharmacology of TAK1 Inhibition by (5z)-7-Oxozeaenol. ACS Chemical Biology. 2012; 8(3):643–50. [PubMed: 23272696]
23. Resch U, Schichl YM, Winsauer G, Gudi R, Prasad K, De Martin R. Siva1 Is a Xiap-Interacting Protein that Balances NF{Kappa}B and JNK Signalling to Promote Apoptosis. Journal Of Cell Science. 2009; 122(15):2651–61. [PubMed: 19584092]
24. Fimia GM, Stoykova A, Romagnoli A, Giunta L, Di Bartolomeo S, Nardacci R, et al. AMBRA1 Regulates Autophagy and Development of the Nervous System. Nature. 2007; 447(7148):1121–5.10.1038/Nature05925 [PubMed: 17589504]
25. Liang C, Feng P, Ku B, Dotan I, Canaani D, Oh B-H, et al. Autophagic and Tumour Suppressor Activity of a Novel Beclin1-Binding Protein UVRAG. Nat Cell Biol. 2006; 8(7):688–98.10.1038/Ncb1426 [PubMed: 16799551]
26. Pomerantz JL, Baltimore D. NF-KB Activation by a Signaling Complex Containing TRAF2, TANK and TBK1, a Novel Ikk-Related Kinase. Embo J. 1999; 18(23):6694–704. [PubMed: 10581243]
27. Huang K, Fingar DC. Growing Knowledge of the mTOR Signaling Network. Seminars in Cell & Developmental Biology. 2014; 36(0):79–90. [PubMed: 25242279]
28. Liang MC, Ma J, Chen L, Kozlowski P, Qin W, Li D, et al. TSC1 Loss Synergizes with Kras Activation in Lung Cancer Development in the Mouse and Confers Rapamycin Sensitivity. Oncogene. 2010; 29(11):1588–97. [PubMed: 19966866]
29. Menon S, Yecies JL, Zhang HH, Howell JJ, Nicholatos J, Harputlugil E, et al. Chronic Activation of mTOR Complex 1 Is Sufficient to Cause Hepatocellular Carcinoma in Mice. Sci Signal. 2012; 5(217):ra24. [PubMed: 22457330]
30. Rao S, Tortola L, Perlot T, Wirnsberger G, Novatchkova M, Nitsch R, et al. A Dual Role for Autophagy in a Murine Model of Lung Cancer. Nat Commun. 2014; 5:3056. [PubMed: 24445999]
31. Pierce AM, Schneider-Broussard R, Gimenez-Conti IB, Russell JL, Conti CJ, Johnson DG. E2F1 Has Both Oncogenic and Tumor-Suppressive Properties in a Transgenic Model. Molecular and Cellular Biology. 1999; 19(9):6408–14. [PubMed: 10454586]

32. Cheung EC, Athineos D, Lee P, Ridgway RA, Lambie W, Nixon C, et al. TIGAR Is Required for Efficient Intestinal Regeneration and Tumorigenesis. Developmental Cell. 2013; 25(5):463–77. [PubMed: 23726973]
33. Lee P, Vousden K, Cheung E. TIGAR, TIGAR, Burning Bright. Cancer & Metabolism. 2014; 2(1):1. [PubMed: 24383451]
34. Morita M, Gravel S-P, Chénard V, Sikström K, Zheng L, Alain T, et al. mTORC1 Controls Mitochondrial Activity and Biogenesis through 4E-BP-Dependent Translational Regulation. Cell Metabolism. 2013; 18(5):698–711. [PubMed: 24206664]
35. Schieke SM, Phillips D, Mccoy JP, Aponte AM, Shen R-F, Balaban RS, et al. The Mammalian Target of Rapamycin (mTOR) Pathway Regulates Mitochondrial Oxygen Consumption and Oxidative Capacity. Journal Of Biological Chemistry. 2006; 281(37):27643–52. [PubMed: 16847060]
36. Egan D, Kim J, Shaw RJ, Guan K-L. The Autophagy Initiating Kinase ULK1 Is Regulated Via Opposing Phosphorylation by AMPK and mTOR. Autophagy. 2011; 7(6):643–4. [PubMed: 21460621]
37. Shimobayashi M, Hall MN. Making New Contacts: The mTOR Network in Metabolism and Signalling Crosstalk. Nat Rev Mol Cell Biol. 2014; 15(3):155–62. [PubMed: 24556838]
38. Dong L-X, Sun L-L, Zhang X, Pan L, Lian L-J, Chen Z, et al. Negative Regulation of mTOR Activity by LKB1-AMPK Signaling in Non-Small Cell Lung Cancer Cells. Acta Pharmacol Sin. 2013; 34(2):314–8. [PubMed: 23178462]
39. Lum JJ, Bauer DE, Kong M, Harris MH, Li C, Lindsten T, et al. Growth Factor Regulation of Autophagy and Cell Survival in the Absence of Apoptosis. Cell. 2005; 120(2):237–48. [PubMed: 15680329]
40. Kim KW, Mutter RW, Cao C, Albert JM, Freeman M, Hallahan DE, et al. Autophagy for Cancer Therapy through Inhibition of Pro-Apoptotic Proteins and Mammalian Target of Rapamycin Signaling. Journal Of Biological Chemistry. 2006; 281(48):36883–90. [PubMed: 17005556]
41. Kwong JQ, Henning MS, Starkov AA, Manfredi G. The Mitochondrial Respiratory Chain Is a Modulator Of Apoptosis. The Journal Of Cell Biology. 2007; 179(6):1163–77. [PubMed: 18086914]
42. Ballot C, Kluza J, Lancel S, Martoriati A, Hassoun S, Mortier L, et al. Inhibition of Mitochondrial Respiration Mediates Apoptosis Induced by the Anti-Tumoral Alkaloid Lamellarin D. Apoptosis. 2010; 15(7):769–81. [PubMed: 20151196]
43. Newman AC, Scholefield CL, Kemp AJ, Newman M, Mciver EG, Kamal A, et al. TBK1 Kinase Addiction in Lung Cancer Cells Is Mediated Via Autophagy of TAX1BP1/NDP52 and Non-Canonical NF-KB Signalling. Plos One. 2012; 7(11):E50672. [PubMed: 23209807]
44. Kim JK, Jung Y, Wang J, Joseph J, Mishra A, Hill EE, et al. TBK1 Regulates Prostate Cancer Dormancy through mTOR Inhibition. Neoplasia. 2013; 15(9):1064–74. [PubMed: 24027431]
45. Zhao B, Li L, Lei Q, Guan K-L. The HIPPO–YAP Pathway in Organ Size Control and Tumorigenesis: an Updated Version. Genes & Development. 2010; 24(9):862–74. [PubMed: 20439427]
46. Tumaneng K, Schlegelmilch K, Russell RC, Yimlamai D, Basnet H, Mahadevan N, et al. YAP Mediates Crosstalk between The Hippo and PI(3)K–TOR Pathways by Suppressing pTEN Via Mir-29. Nat Cell Biol. 2012; 14(12):1322–9.10.1038/Ncb2615 [PubMed: 23143395]
47. Dovey JS, Zacharek SJ, Kim CF, Lees JA. BMI1 Is Critical for Lung Tumorigenesis and Bronchioalveolar Stem Cell Expansion. Proceedings Of The National Academy Of Sciences. 2008; 105(33):11857–62.
48. Liu J, Cao L, Chen J, Song S, Lee IH, Quijano C, et al. BMI1 Regulates Mitochondrial Function and the DNA Damage Response Pathway. Nature. 2009; 459(7245):387–92.10.1038/Nature08040 [PubMed: 19404261]
49. Voigt, W. Sulforhodamine B Assay and Chemosensitivity. In: Blumenthal, R., editor. Chemosensitivity. Humana Press; 2005. p. 39-48.
50. Subramanian A, Tamayo P, Mootha VK, Mukherjee S, Ebert BL, Gillette MA, et al. Gene Set Enrichment Analysis: A Knowledge-Based Approach for Interpreting Genome-Wide Expression Profiles. Proceedings Of The National Academy Of Sciences. 2005; 102(43):15545–50.

Significance

These findings collectively reveal a novel role for the p53 target gene *Siva* both in regulating metabolism and in enabling tumorigenesis, independently of p53. Importantly, these studies further identify SIVA as a new prognostic marker and as a potential target for NSCLC cancer therapy.

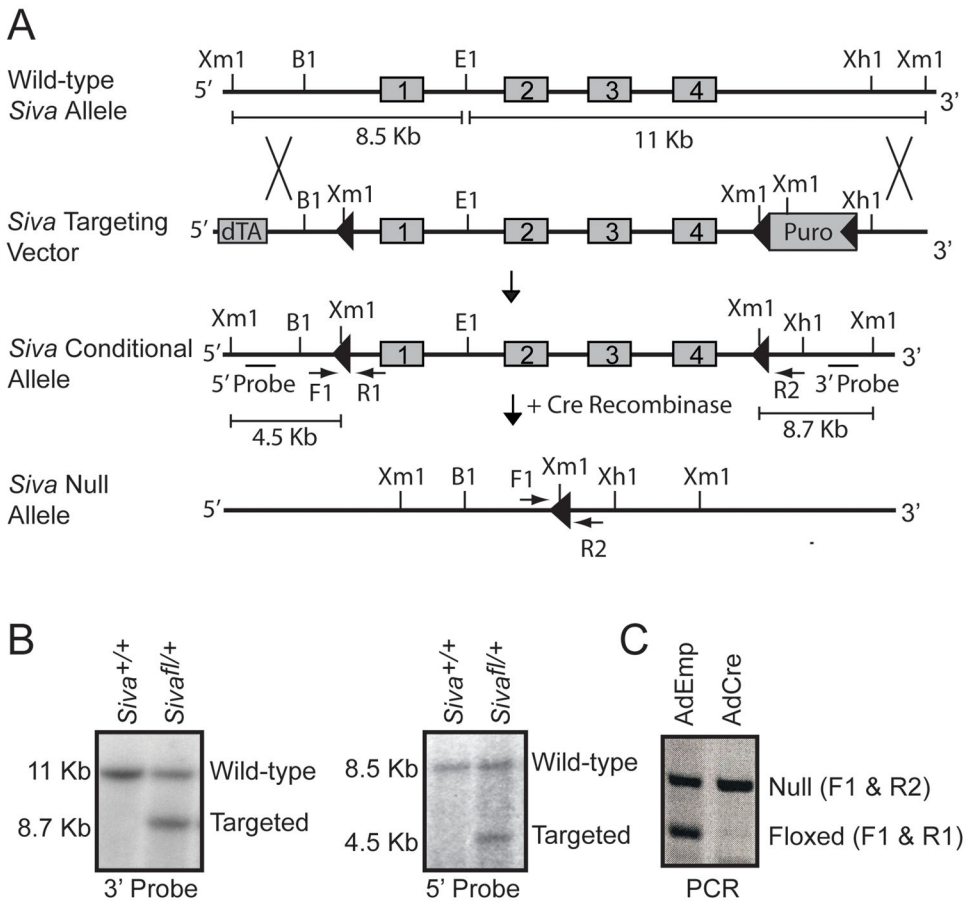

Figure 1. Generation of *Siva* Conditional Knockout Mice

A) Targeting scheme for generating *Siva* conditional knockout mice. The *Siva*-targeting vector contains a positive selection marker (Puromycin cassette (Puro)) flanked by *loxP* sites (triangles) and a negative selection marker (diphtheria toxin (dTA)). The four exons comprising the *Siva* locus (grey boxes) are flanked by LoxP and Lox-Puro-Lox sites on the 5′ and 3′ ends, respectively. The Puro cassette was removed *in vivo* by limited Cre expression, leaving a single 3′ LoxP site. Upon subsequent Cre recombinase expression, the *Siva* locus gets excised, resulting in a *Siva* null allele. These recombination events were detected by Southern blot analysis using Xmn1/EcoR1 restriction digests and subsequent probing with a 5′ or 3′ fragment external to the targeting vector. This leads to generation of fragments of different sizes in all cases, as shown. B1: BamH1, E1: EcoR1, Xm1: Xmn1, Xh1: Xho1 B) Southern blot analyses of mouse embryonic stem cells targeted at the *Siva* locus. Analyses of a wild-type ($Siva^{+/+}$) and a targeted ($Siva^{fl/+}$) ES cell clone are shown. DNA was digested with Xmn1/EcoR1. Left: Upon probing with the 3′ probe, the 11 Kb band indicates the wild-type allele and the 8.7 Kb band indicates the targeted conditional allele. Right: Upon probing with the 5′ probe, the 8.5 Kb band indicates the wild-type allele and the 4.5 Kb band indicates the targeted conditional allele. C) PCR analysis of recombined allele. Mouse embryonic fibroblasts generated from E13.5 $Siva^{fl/-}$ embryos (where fl denotes the conditional knockout allele) were infected either with Adenovirus expressing Cre (Ad-Cre) to excise the *Siva* floxed allele or with empty Adenovirus (Ad-Emp) as a

control. Primers spanning the 5′ LoxP site (F1 and R1) or the remaining LoxP site after excision of the *Siva* locus (F1 and R2) were used. The absence of the floxed allele following Ad-Cre infection verifies the ability of Cre to fully excise the *Siva* locus.

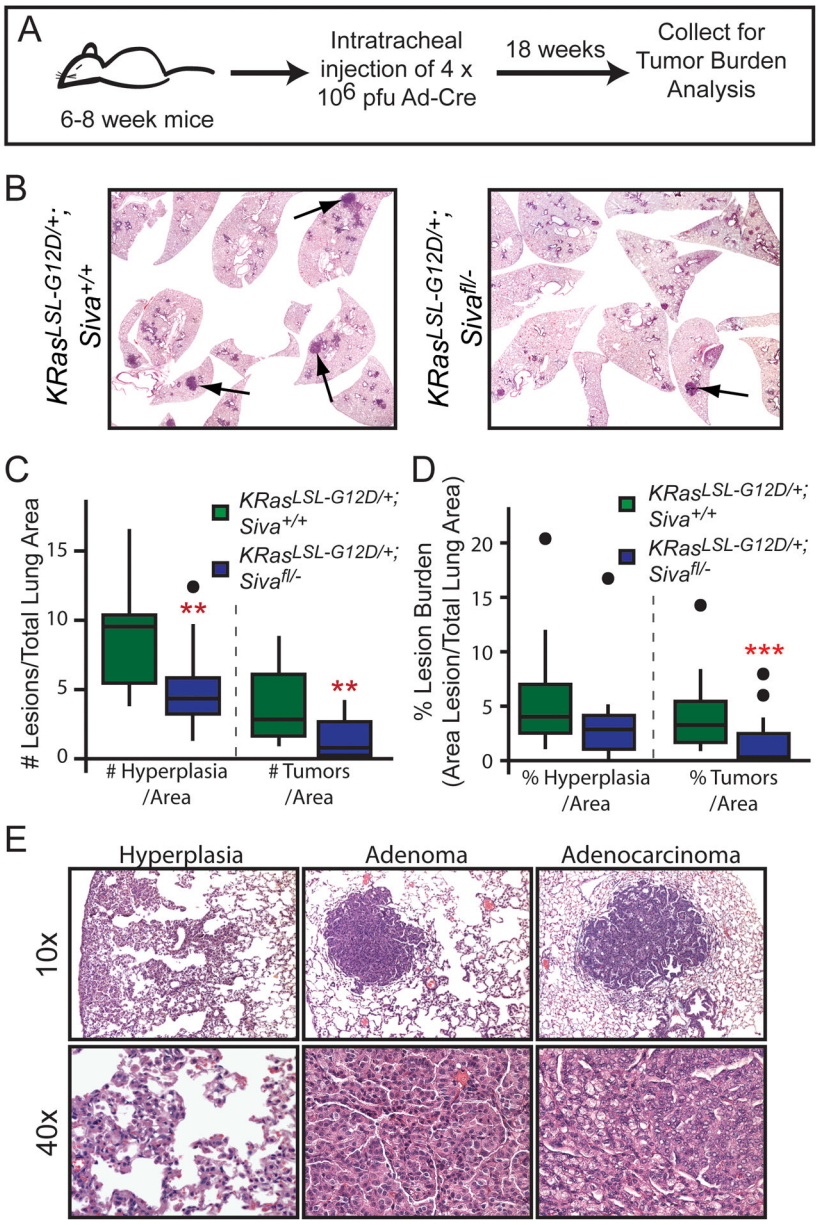

Figure 2. *Siva* Deficiency Inhibits Lung Tumorigenesis

A) Schematic of the timeline for tumor study. 6–8 week old mice were infected with Ad-Cre via intratracheal injection, and lungs were analyzed 18 weeks later. B) Representative photomicrographs of lungs from $Kras^{LSL\text{-}G12D};Siva^{+/+}$ (left, n=12) and $Kras^{LSL\text{-}G12D};Siva^{fl/-}$ (right, n=17) mice 18 weeks after Ad-Cre infection by intratracheal injection. C) Boxplot depicting the median number and quartiles of hyperplasias and tumors (adenomas and adenocarcinomas) per total lung area in $Kras^{LSL\text{-}G12D};Siva^{+/+}$ and $Kras^{LSL\text{-}G12D};Siva^{fl/-}$ mice. Dots represent outlier data points. Hyperplasias: **p=0.008; Tumors **p=0.0058 by Wilcox Rank Sum Test between $Kras^{LSL\text{-}G12D};Siva^{+/+}$ and $Kras^{LSL\text{-}G12D};Siva^{fl/-}$ mice. D) Boxplot depicting median tumor burden and quartiles calculated as tumor area per total lung area for hyperplasias and tumors (adenomas and

adenocarcinomas). Dots represent outlier data points. Hyperplasia p=0.066; Tumor ***p= 0.003 by Wilcox Rank Sum Test between *Kras*$^{LSL\text{-}G12D}$;*Siva*$^{+/+}$ and *Kras*$^{LSL\text{-}G12D}$;*Siva*$^{fl/-}$ mice. E) Representative photomicrographs of hyperplasias and tumors (adenomas and adenocarcinomas) taken at 100x and 400x magnification.

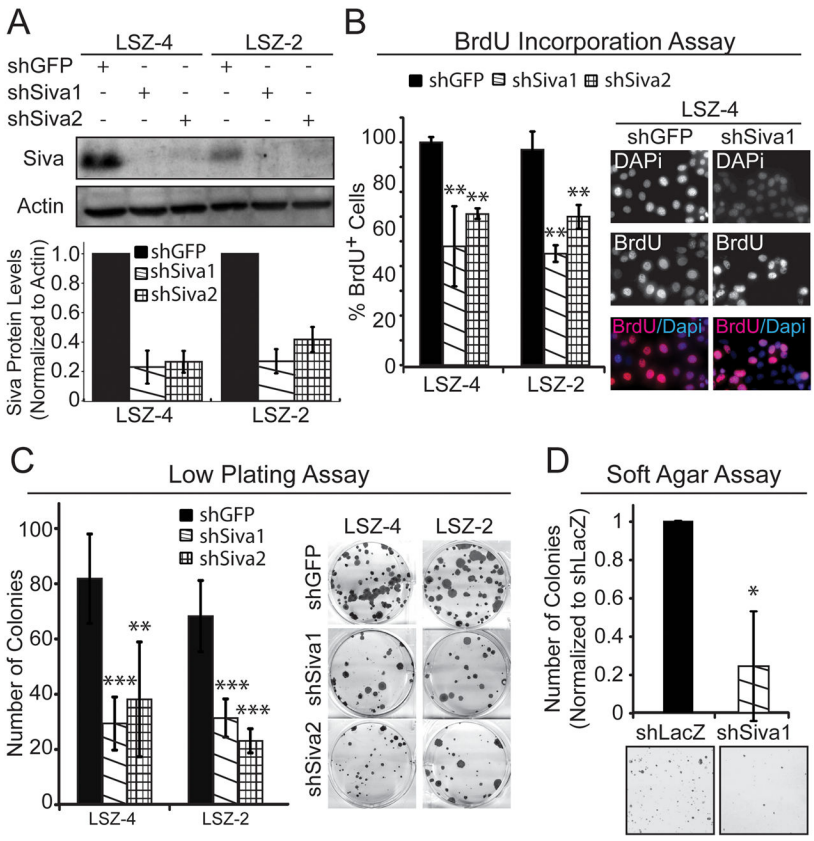

Figure 3. *Siva* Knockdown Inhibits Cellular Proliferation and Transformation in Mouse Non-Small Cell Lung Cancer Cells

A) (Top) Western blot analysis of SIVA in LSZ4 and LSZ2 Non-Small Cell Lung Cancer (NSCLC) cell lines. Two independent shRNAs targeting SIVA were used to knock-down SIVA. shRNA targeting GFP was used as a negative control. ACTIN serves as a loading control. (Bottom) Quantification of SIVA protein levels following expression of two *Siva* shRNAs compared to expression of shGFP, after normalization to ACTIN. B) (Left) Average percent BrdU incorporation upon *Siva* knockdown in LSZ4 and LSZ2 cells compared to control knockdown with shGFP. Error bars represent +/−SD. p-values by Student's t-test comparing each shRNA to shGFP: LSZ4: **p=0.006, 0.002; LSZ2: **p=0.003, 0.007 (Right) Representative images of BrdU immunofluorescence. Blue: DAPI; Red: BrdU. C) (Left) Average number of colonies in low plating assay upon *Siva* knockdown in LSZ4 and LSZ2 cells compared to control knockdown with shGFP. Error bars represent +/−SD. p-values by Student's t-test: LSZ4: ***p=0.0002; **p=0.0025; LSZ2: ***p=0.0004, 0.0001. (Right) Representative images of colonies in low plating assay stained with crystal violet. D) (Top) Average number of colonies in soft agar assay upon *Siva* knockdown in LSZ4 cells relative to control knockdown with shLacZ. Error bars represent +/−SD. *p-value by Student's t-test: 0.047 (Bottom) Representative images of colonies in soft agar assay stained with Giemsa.

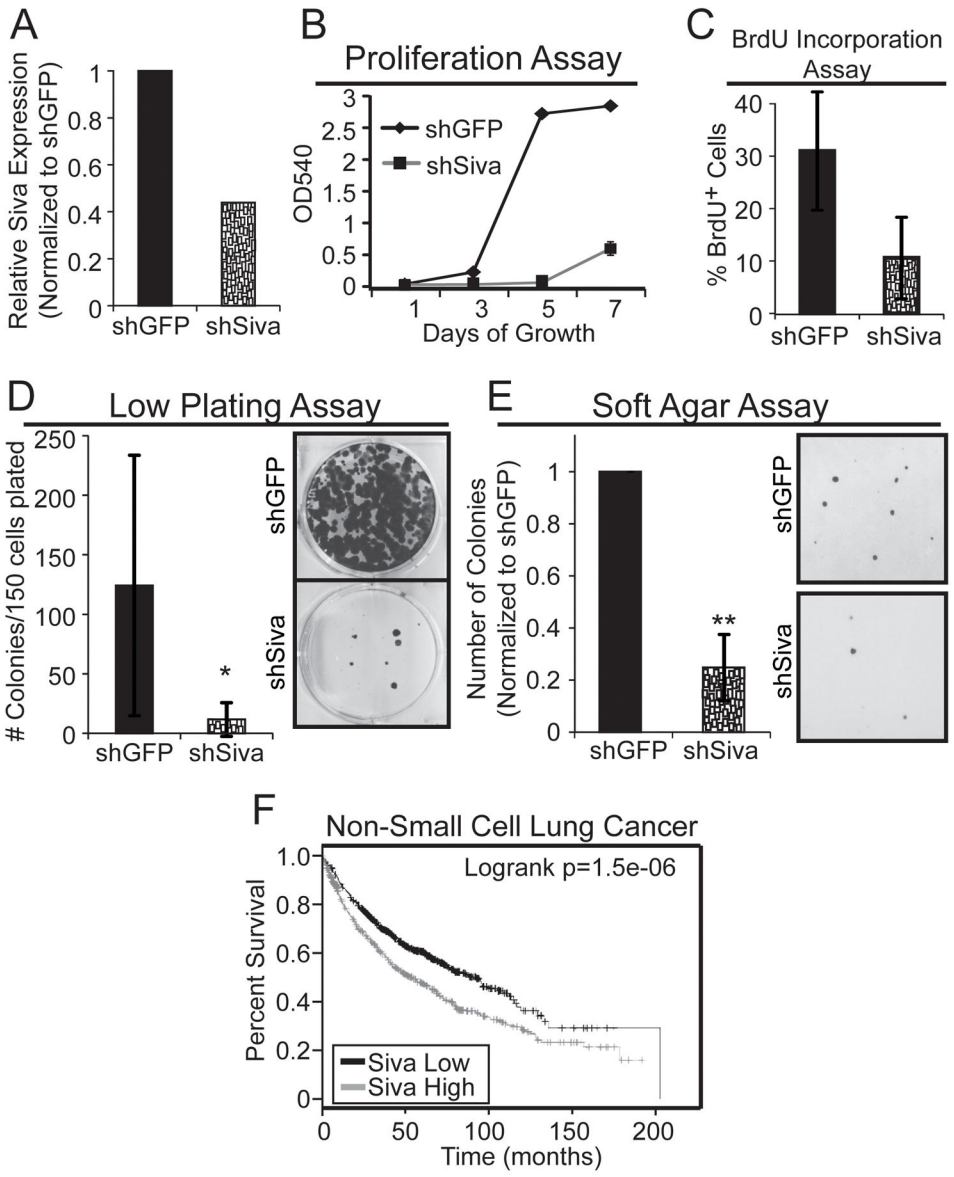

Figure 4. *SIVA* Knockdown Inhibits Cellular Proliferation and Transformation in Human Non-Small Cell Lung Cancer Cells

A) *SIVA* expression in A549 cells, as assessed by quantitative RT-PCR normalized to *β-ACTIN*, upon expression of shRNA targeting *SIVA* or shRNA targeting GFP. B) Representative cellular proliferation assay in A549 cells over 7 days following *SIVA* or control GFP shRNA transduction. The experiment was repeated in duplicate with two independent shRNAs to *SIVA* each time. C) Average percent BrdU incorporation in *SIVA*-knockdown cells. Error bars represent +/−SD. p-value by Student's t-test: 0.058. D) (Left) Average number of colonies in low plating assay following *SIVA* or control GFP shRNA transduction. Error bars represent +/−SD. (Right) Representative images of colonies in low plating assay stained with crystal violet. *p-value by Student's t-test: 0.05. E) (Left) Average number of colonies in soft agar assay upon knockdown of *SIVA* relative to control cells expressing shGFP. Error bars represent +/−SD. **p-value by Student's t-test: 0.0013.

(Right) Representative images of soft agar assay stained with Giemsa. F) Survival Curve from human Non-Small Cell Lung Cancer Patients generated using KMplot.com and gene expression from the *SIVA1* probe 203489_at. *SIVA* expression levels: Low – Black; High – Red.

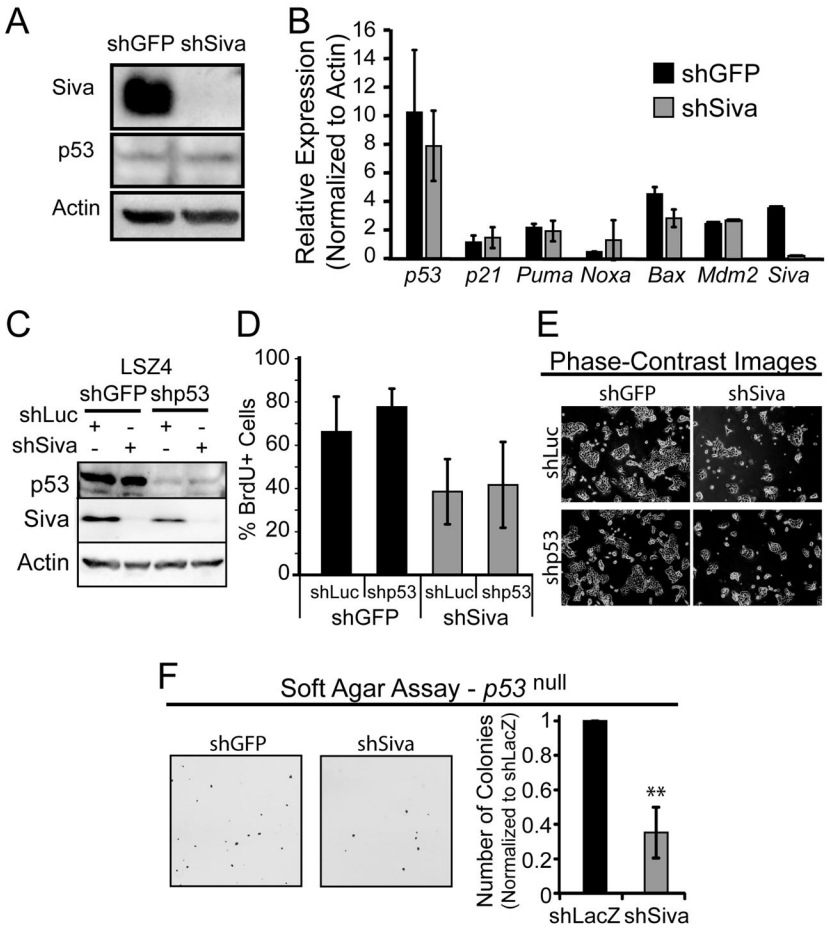

Figure 5. Phenotypes Induced by *Siva* Knockdown are p53-Independent

A) Western blot analysis of p53 levels upon *Siva* knockdown in LSZ4 cells. Western blot analysis for SIVA shows knockdown with shSiva relative to shGFP. ACTIN serves as a loading control. B) qRT-PCR analysis of p53 target gene expression, after normalization to *β-actin*, in NSCLC cells transduced with shSiva or shGFP. Error bars represent +/−SD. n=2. C) Western blot analysis of p53 and SIVA upon knockdown of *p53* and/or *Siva* in LSZ4 cells. ACTIN was used as a loading control. D) Average of percent BrdU incorporation in LSZ4 cells upon knockdown of *p53* and/or *Siva*. shGFP and shLuc served as controls. Error bars represent +/−SD. n=3. E) Phase-contrast images of LSZ4 cells upon knockdown of *p53* and/or *Siva*. F) (Left) Images of colony formation in soft agar assays performed in *p53* null NSCLC cells with knockdown of *Siva*. (Right) Average number of colonies formed relative to shLacZ transduced cells in soft agar assays. Error bars represent +/−S.D. n=3.

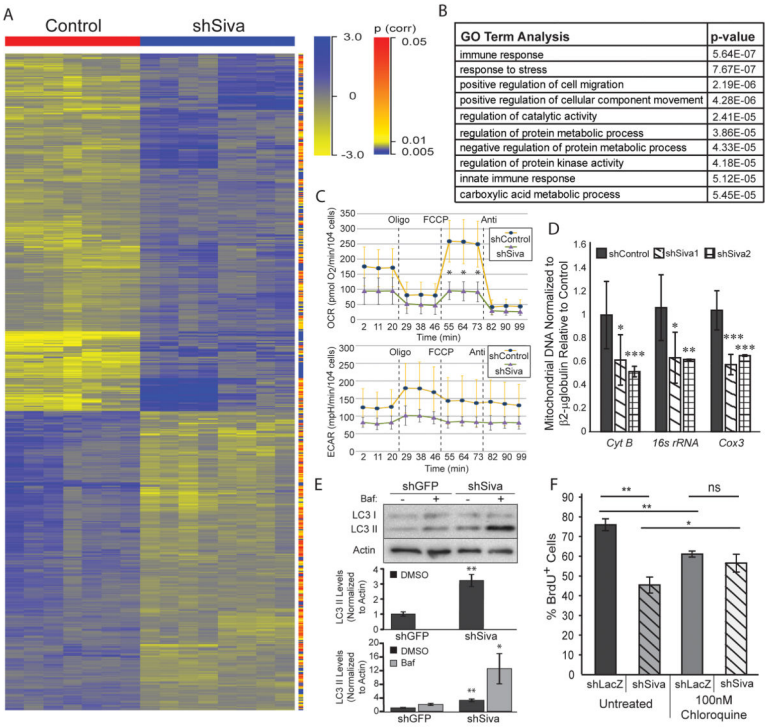

Figure 6. SIVA loss decreases metabolic function of NSCLC cells

A) Heat map of gene expression based on hierarchical clustering of microarray data from LSZ2 and LSZ4 cells with control knock-down using two control hairpins (shGFP and shLacZ) (Red) or knock-down of *Siva* using two independent hairpins (shSiva1 and shSiva2) (Blue). Genes identified for the heat map were significantly modulated (p-value less than or equal to 0.05) and had a fold change equal to or greater than 1.5. Yellow signifies downregulated genes while Blue signifies upregulated genes. p-value for each gene is denoted on the right hand side with either red (high) or blue (low) bars. B) GO Term analysis of genes with altered expression upon *Siva* shRNA transduction into LSZ2 and LSZ4 cells relative to cells with control shRNA transduction. The p-value for each category is shown on the right side. GO term analysis was performed using GeneSpring-GX software (Agilent). C) Oxygen consumption rate (OCR) and extracellular acidification rate (ECAR) in LSZ4 cells upon *Siva* knockdown or in *shGFP* transduced control cells. Oligo: oligomycin (ATP synthase inhibitor [electron chain inhibitor]), FCCP (uncoupler), Anti: antimycin (electron gradient disrupter). *p-value by Student's t-test: 0.024 D) Mitochondrial DNA content assessed by quantitative PCR for mitochondrial-encoded genes upon knockdown of *Siva* in LSZ4 cells and in shGFP transduced control cells. Normalized to *β2-microglobulin*. E) (Top) Western blot analysis of autophagy related protein LC3-II in LSZ4 cells upon shSiva or shGFP control transduction. ACTIN used as a loading control. (Bottom) Quantification of LC3-II levels upon *Siva* knockdown without (top) and with Bafilomycin A1 (bottom), relative to *β*-ACTIN. p-value by Student's t-test: *0.05, **0.007. F) Average percent BrdU incorporation in LSZ-4 cells with control (shLacZ) or *Siva* (shSiva) knockdown in the absence (untreated) or presence of chloroquine. Cells were incubated with 100nM chloroquine for 18 hours prior to BrdU pulse. Graph represents

average +/− SD of three experiments. *p-value<0.05; **p-value<0.01; ns: not significant by Student's t-test. n=3.

A

GSEA Analysis	FDR	NES
BMI1_DN_MEL18_DN.V1_UP	0.000932	2.05
KRAS.DF.V1_DN	0.0138	1.98
RB_DN.V1_DN	0.0122	1.96
HOXA9_DN.V1_UP	0.0213	1.89
YAP_CONSERVED_SIGNATURE	0.0344	1.83
AKT_UP_MTOR_DN.V1_UP	0.0392	1.81
BMI1_DN.V1_UP	0.0436	1.79
PTEN_DN.V1_UP	0.0453	1.77
RPS14_DN.V1_UP	0.0422	1.77
E2F1_UP.V1_DN	0.0514	1.74

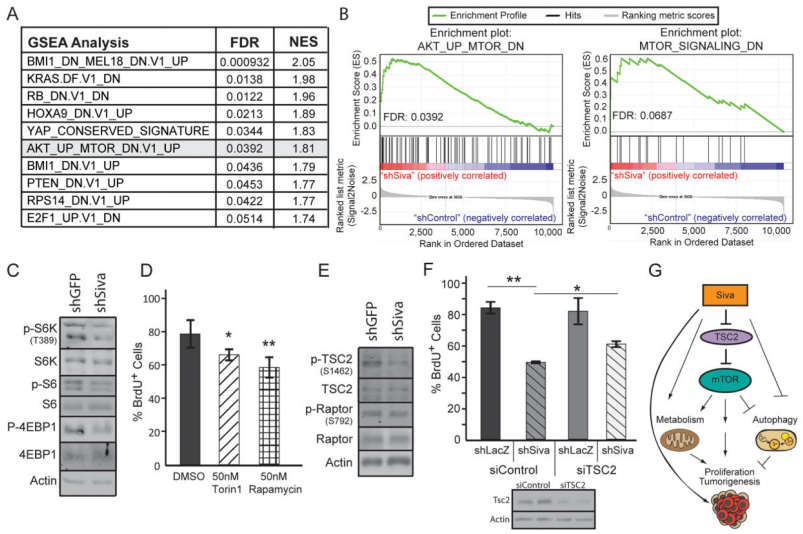

Figure 7. SIVA loss decreases metabolic function of NSCLC cells

A) Gene Set Enrichment Analysis (GSEA) of genes with altered expression upon *Siva* shRNA transduction into LSZ2 and LSZ4 cells relative to cells with control shRNA transduction. The FDR p-value and normalized enrichment score (NES) for each category are shown on the right side. The GSEA signature for decreased mTOR signaling is highlighted in grey. B) Select GSEA profiles (Left) Enrichment of genes upregulated upon mTOR inhibition in the presence of AKT upregulation. FDR q-value: 0.039 (Right) Enrichment of genes downregulated upon mTOR activation. FDR q-value: 0.069 C) Western blot analysis of mTOR signaling targets in LSZ4 cells upon shSiva or shGFP control transduction. ACTIN serves as a loading control. D) Average percent BrdU incorporation in LSZ-4 cells treated with 50nM Torin1 or 50nM Rapamycin for 18 hours. Error bars represent +/−SD. p-value by Student's t-test: *Torin1: 0.048; **Rapamycin: 0.009. E) Western blot analysis of mTOR upstream signaling components in LSZ4 cells upon shSiva or shGFP control transduction. ACTIN serves as a loading control. F) Average percent BrdU incorporation in LSZ-4 cells with control (shLacZ) or *Siva* (shSiva) knockdown and without (siControl) or with TSC2 (siTSC2) knockdown. Error bars represent +/−SD *p-value<0.05; **p-value<0.01 by Student's t-test. G) Model depicting the role of SIVA in promoting tumorigenesis through activation of mTOR signaling, which can itself affect metabolism, proliferation, tumorigenesis and autophagy. SIVA may also have mTOR-independent effects on these processes.